From Chemical Drawing to Electronic Properties of Semiconducting Polymers in Bulk: A Tool for Chemical Discovery

Colm Burke[1], Hesam Makki[1], Alessandro Troisi*

[1]Department of Chemistry and Materials Innovation Factory, University of Liverpool, Liverpool L69 7ZD, U.K.

Corresponding Author:
Hesam Makki
Email: h.makki@liverpool.ac.uk

Abstract

A QC/MD scheme is developed to calculate electronic properties of semiconducting polymers in three steps: (i) constructing the polymer force field through a unified workflow, (ii) equilibrating polymer models, and (iii) calculating electronic structure properties (e.g., density of states and localisation length) from the equilibrated models by quantum chemistry approaches. Notably, as the second step of this scheme, we introduce an alternative method to compute thermally averaged electronic properties in bulk, based on the simulation of a polymer chain in the solution of its repeat units, which is shown to reproduce the microstructure of polymer chains and their electrostatic effect (successfully tested for five benchmark polymers) ten times faster than state-of-the-art methods. In fact, this scheme offers a consistent and speedy way of estimating electronic properties of polymers from their chemical drawings- thus, ensuring the availability of homogenous set of simulations to derive structure-property relationships and material design principles. As an example, we show how the electrostatic effect of polymer chain environment can disturb the localized electronic states at the band tails and how this effect is more significant in case of diketopyrrolopyrrole polymers as compared to indacenodithiophene and dithiopheneindenofluorene ones.

1. Introduction

Semiconducting polymers (SCPs) are one of the main classes of organic electronics materials able to display both high charge carrier mobility (up to 20 cm^2 V^{-1} s^{-1}) and excellent mechanical flexibility,[1,2] putting them forward as a great candidate for flexible electronics.[3] Moreover, the modular approach to their synthesis lends itself to a natural approach to molecular design,[4] namely the selection of a sequence of conjugated fragments and sidechains in the repeat unit structure for a targeted application, e.g., organic photovoltaics,[5] field effect transistors,[6] light emitting diodes,[7] and bioelectronics,[8] based on their optical, electronic, thermal, and mechanical properties.

The design rules, which are prerequisite for the molecular design, naturally emerge from structure-property datasets obtained from a homogenous study of many compounds. Computational studies of many SCPs can lead to structure-property relationships in the same way as typically done for small-molecule organic electronics.[9] In this line, quantum chemistry (QC) methods have shown notable success in screening and discovery of small-molecule organic electronics based on desired electronic properties.[10] For instance, they enabled the discovery of extremely rare organic electronic compounds,[11,12] unravelled the effect of molecular chirality on their opto-electronic properties,[13] and established (sometimes rather counterintuitive) design principles.[14] Also, similar well-established QC methods are available to calculate electronic properties of SCPs, e.g., through the calculation of density of states (DOS)[15] and by employing model reduction methods.[16] Recent advances in the automation of such calculations shows that a great insight into the design rules can be obtained by considering medium-to-large size datasets of SCPs.[17] However, so far, high-throughput methods have been only reserved for single polymer chains in vacuum or implicit solvents,[18–21] missing the (undeniable) role of intermolecular interactions on polymer conformation and the electrostatic effect of the surrounding polymer chains in bulk.

Molecular dynamics (MD) is an ideal method to construct high-quality SCP bulk models,[22–28] from which one can include the intermolecular and electrostatic effects of the environment in electronic properties calculations through a hybrid QC/MD method.[15] Such an approach consists of three main steps: (i) model construction, (ii) equilibration of the models, and (iii) QC calculations on the equilibrated models. The first step suffers from inconsistencies, due to the various choices adopted for different force field parametrisation methods, e.g., explicit,

or implicit ways of determining the equilibrium value of bonded parameters or atomic charges, and is often a tedious and laborious step, because of the many parameters such models require. The second step is generally the most time consuming one, due to the long relaxation times of SCPs, which often scales unfavourably with the molecular weight[29]. Also, there is no commonly accepted equilibration method due to the rather different microstructures of SCPs, e.g., from semi-crystalline polymers to amorphous glasses, and the wide range of glass transition temperature T_g (or melting points) for different SCPs[30]. With respect to the third step, many alternatives are available including semiempirical,[31,32] tight binding,[33,34] and DFT methods,[15,35] which reduce the comparability between different works. The aforementioned inhomogeneities and implemental difficulties resulted in studying a limited number of models, i.e., only a few high-quality polymer models per investigation has been possible.[36,37] Thus, having fewer models studied and incomparable models generated in different studies has obstructed the development of structure-(electronic) property relationships required for formulating SCP design rules. Therefore, developing consistent and standardized SCP models, able to provide accurate electronic structures for a variety of polymers and a reasonable computational cost will offer a great foundation for the application of digital discovery approach to the class of SCPs.

In this paper, we put forward (i) a unified workflow to develop chemical-drawing-to-atomistic models for SCP chains and (ii) an accelerated approach to obtain electronic structure properties, which takes into account the inter-molecular interactions and electrostatic environment of the surrounding chains. The accuracy of the QC/MD method is evaluated by comparing the morphological characteristics (e.g., torsion angle distribution, end-to-end distance, radial distribution function,) and electronic properties (e.g., DOS and DOS-driven properties), calculated for polymer chains sampled from (conventionally) equilibrated polymer melt models and those constructed by the faster alternative approach.

2. Method

2.1. A workflow to develop drawing-to-atomistic models

Scheme 1 shows a unified workflow for generating the SCP chain models. As shown, the conjugated monomers and their sequence in the polymer repeat unit are given as the input. One cannot assume that the net charge on each monomer to be exactly zero (we have noticed up to |0.08|e shifting between monomers), i.e. the parameters of the individual monomer

are not transferable, and the parametrisation is best carried out using a larger model. We have considered here a minimal model where the repeat unit is capped with the first and last monomers and alkyl sided chains are replaced by methyl terminations (shown in step 1 of scheme 1). This model was used to compute the force field parameters including atomic point charges and bonded equilibrium parameters through DFT calculations (in this case B3LYP/6-31G*). The model of this size will also alleviate the possible dependency of the inter-monomer torsional potential upon the neighbouring monomers or the length of oligomer structure as observed before.[38] We identified the lowest energy conformer for the model oligomer by exhaustive search of all possible cis/trans configuration. Then, a universal DFT-based protocol is used to calculate the intra- and inter-fragment force field parameters (steps 2 and 3 in scheme 1), see SI, sections S1.1 and S1.2 for details. It should be noted that an important feature of this workflow is that each individual intra-fragment bond, angle, and torsion angle equilibrium value is directly taken from the DFT-optimised minimal model, meaning that they are not only determined by the atom types forming the bond/angle/torsion- as is the case in generalised force fields such as OPLS-FF[39] and GAFF[40], but the entire minimal model structure. This explicit method for bonded parameter calculation maintains the relative atomic positions (within each monomer) close to the real conjugated monomer structure during MD simulations. This feature is essential for the expected accuracy in calculating the electronic structures of SCP models (made by MD) due to the significance of relative atomic positions on the molecular orbital.[41–44] The choice for DFT functional/basis set (in this version: B3LYP/6-31G*) was made to be consistent with the follow-up QC calculations which will be done directly on the MD snapshots as explained in section 2.3. Also, note that the workflow is designed to be adaptable, should different density functional or parent force field become desirable. The key point is that the protocol and choices are made once to be used consistently for all polymers modelled in one study.

After calculating the force field parameters for the minimal model (representing the backbone of the polymer), the sidechains are attached to the designated positions, i.e., all methyl groups in the minimal polymer model, the sidechain force field parameters (united-atom and directly taken from OPLS-FF) are added, and the atomic charges around the sidechain-backbone connection points are corrected to maintain the whole repeat-unit charge neutrality (step 4 in scheme 1), see SI, sections S1.3 and S1.4. Last, polymer chain models (i.e., coordinates and

force field files) with desired degrees of polymerisation (e.g., in this study n = 10 since the effect of M_w on the calculated electronic structure properties was found to be negligible[27] from n ≥ 10) are generated (step 5 in scheme 1). Note that the Lennard-Jones parameters for all backbone atoms were also taken from OPLS force field to be consistent with the sidechain parameters.

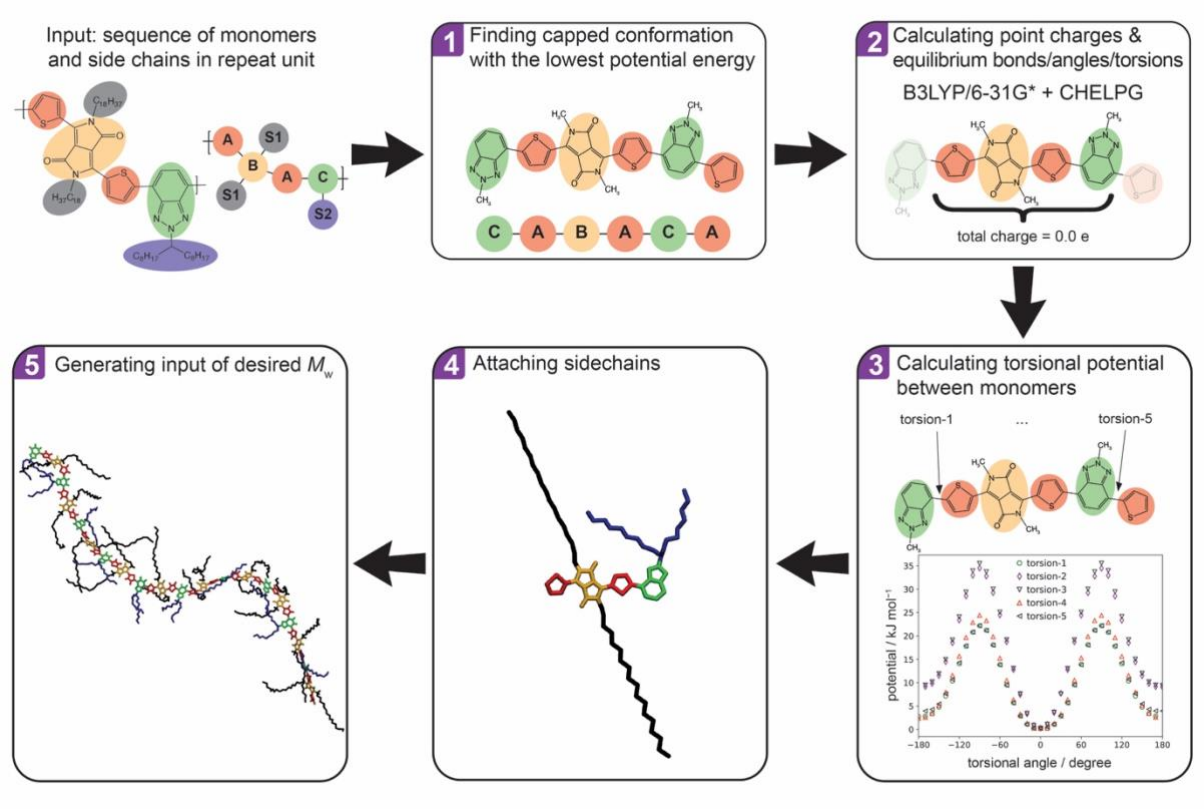

Scheme 1. The workflow for generating SCP chain models from their chemical drawings.

2.2. A simplified surrogate for MD equilibration of the models

We used two methods for SCP model equilibration in this paper: (i) conventional method: a well-established equilibration protocol for SCPs (i.e., performing several annealing cycles, each includes above-T_g / just-below-T_g / room-temperature equilibration[26,27,45,46]), to which we refer as "melt" for the rest of the manuscript, and (ii) a faster surrogate method: equilibrating one SCP chain in the soup of its repeat units at a temperature well above repeat unit melting point (i.e., 900 K, see SI, section S2.1). This is an approximation of the ideal solvent for the chain, and we can hypothesise that it represents similar intermolecular interactions and electrostatic disorder. These hypotheses will be tested by comparison with the "melt" simulations for five different SCPs shown in Figure 1a (all of which are benchmark polymers belong to the new generation of non-semicrystalline SCP family). We will refer to this method

as the “soup” for the rest of the manuscript. Examples of equilibrated simulation boxes for both “melt” (i.e., 50 polymer chains in a cubic box) and “soup” (i.e., one polymer chain and 300 repeat units in a rectangular box with approximately 4:1:1 aspect ratio) methods are shown in Figure 1c. Note that in case of “soup”, the polymer chain is initially aligned with the largest dimension of the rectangular box (i.e., x axis) so that a lower number of pseudo-solvent molecules (i.e., in our case the repeat unit of polymer) is needed compared to a cubic box. It is worth noting that by changing the number of pseudo-solvents from 150 to 600, we noticed that from 200 molecules onward, the microstructural properties of the polymers (e.g., end-to-end distance) converge.

To equilibrate SCPs through “melt” method, the T_g of SCP model is essential for the simulation setting. Estimating T_g through MD simulations strongly depends on the calculation method[47] due to the several factors, e.g., extremely high simulation cooling/heating rates, different fitting procedures, and considerably wide range of transition region. In this work, we used two different methods to estimate the T_g of the SCP models and we observe up to 300 K difference in the calculated values obtained from density-temperature and mean squared displacement (MSD)-temperature graphs, both from the same temperature-sweep simulation trajectories (see SI, section S2.1). For our “melt” simulation settings, we used the values obtained from MSD curves as they give a direct estimation of the temperature at which a clear increase in the dynamics of polymer chains occurs. Thus, 1200 K was chosen to anneal all SCP models above their T_g and a temperature between 700-850 K (depending on the polymer type) for sub-T_g relaxations was used (see SI, Figure S11). This emphasises on another advantage of the “soup” method in which a constant high temperature (i.e., 900 K which is well above the melting points of all repeat units) can be used for any SCP and the T_g estimation step (which is a prerequisite to the conventional “melt” equilibration) can be avoided.

For both “melt” and “soup” methods, after energy minimisation a rapid contraction of the box was done (under NPT and with P = 1000 bar) to quickly pack the box to the correct density. Equilibration simulations were done under NPT conditions with a time step of 2 fs using GROMACS. A mass rescaling method for the backbone hydrogen atoms is employed to enable using larger time steps during MD equilibration.[48] A 1.0 nm cutoff for Lennard-Jones and electrostatic interactions was used and all nonbonded interactions for 1-2 and 1-3 bonded pairs were excluded and a scaling factor of 0.5 was used for 1-4 bonded pairs. V-rescale

thermostat and C-rescale barostat were used for packing steps and the Nose-Hoover thermostat and Parrinello-Rahman barostat were employed for equilibration runs. Verlet cut-off scheme was employed for non-bonded interactions and Particle-mesh Ewald was used for long-range electrostatic interactions. Examples of coordinate, topology, and run files can be found in https://github.com/HMakkiMD/QCMD.

We previously verified the quality of the models generated by the workflow shown in scheme 1 and equilibrated through "melt" method for IDT-BT, where a strong agreement between the simulated X-ray scattering patterns from our models and the pattern given by GIWAXS measurement was achieved, see Figure 2 in ref.[27] Similar analyses on the microstructures of two DPP-based (i.e., DPP-2TT and DPP-DTT) and two BT-based (i.e.. IDT-BT and TIF-BT) models obtained from "melt" equilibration has been done and a comparison with experimental data is discussed in section 2.2 of the SI, demonstrating that a single workflow can be successfully validated across a class of materials.

2.3. QC calculations for a chain in the "shell" of its repeat units

For each polymer, we sampled 250 chains, which are all statistically independent according to the block averaging analysis performed on SCP chain lengths, as shown and discussed in SI, section S2.3. The electronic structure (orbital energies and localization) for each chain was computed taking into account their electrostatic environment (included via the point charges of all repeat units which have at least one atom within 2 nm distance from any atom in the polymer backbone) from both "melt" and "soup" simulation trajectories (see Figure 1c). These calculations are sped up with negligible loss of accuracy[49] by using the smaller 3-21G* basis set and the same functional (B3LYP) used to derive the force field parameters. The DOS of each sample was calculated (see the QC calculation details in ref[15]) and averaged over 250 chains. It should be noted that in p-type organic semiconductors (including all the SCPs investigated in this paper), the shape of the DOS, particularly the distribution of states at the valence band edge, is closely tied to electronic disorder and hence charge mobility[3,36,50]. Quantifying this, for example, via the slope of the valence band tail or by the charge carrier localisation length (LL) at the valence band edge provides a valuable link between electronic structure calculation and experimentally measurable quantities, e.g., mobility.

Considering the smaller number of atoms in simulation box, the extremely faster equilibration, and the exemption of T_g calculation for "soup" method, obtaining 250

independent samples for QC calculations takes on average one tenth of the computation time needed for the "melt" method. It should be noted that we used 20 annealing cycles for equilibration through "melt" approach to cover a homogenous setting for all polymers in this study (see SI, section 2.2); however, the number of cycles needed for different polymers varies based on their relaxation time spectra and needed to be determined each individual polymer by monitoring its properties during equilibration. This shows another advantage of the "soup" method, for which we use one simulation setting for any polymer at hand without monitoring its properties during equilibration. In Table 1, we summarised the computational cost, including the force field generation, MD equilibration, and QC calculations, for the "melt" and "soup" methods to achieve the same statistical sampling. In fact, this analysis shows that by employing the workflow for SCP model generation (shown in scheme 1), the calculation (including the investigator) time has been tremendously decreased (from typically a few months per polymer per investigator to below two weeks per polymer per computer node) so that the "melt" method is reasonably suitable to investigate electronic structure properties of any polymer of interest as well as several polymers in one investigation. Moreover, the "soup" method (with total calculation time of around 1-2 days per polymer per computer node) can be pushed to become a discovery tool where a large number (e.g., hundreds) of hypothetical models are explored in one study.

Table 1. The computational time of "melt" and "soup" QC/MD methods considering the five SCPs discussed in this paper. Note that similar GPU- and CPU- computer nodes (one Nvidia A40 GPU/AMD EPYC 7443 CPU and one Intel(R) Xeon(R) Gold 6230, for MD and QC calculations, respectively) were used for all polymers through "melt" and "soup" methods.

	Force field parametrisation	MD equilibration	QC calculations	total
"Melt" method	6-10 h	8-12 day	8-10 h	9-13 day
"Soup" method	6-10 h	10-14 h	8-10 h	1-2 day

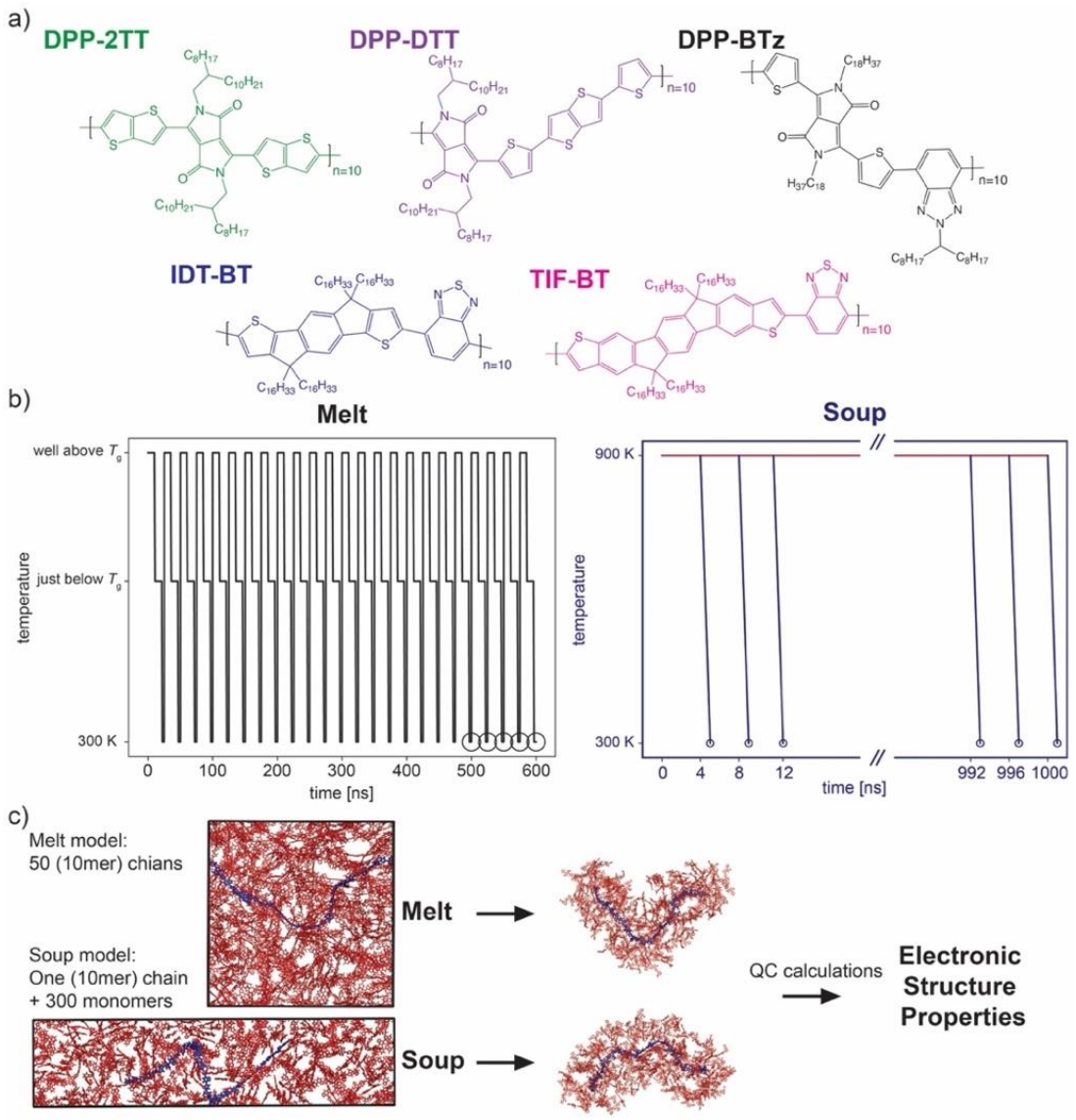

Figure 1. a) Polymer structures. b) Equilibration scheme for "melt" vs "soup" methods. Each large circle in "melt" graph represents 50 chains sampled from one snapshot (therefore 50 x 5 = 250 samples in total), and each small circle in "soup" graph represents one chain sampled from one snapshot (therefore, 1 x 250 = 250 samples in total. c) Input generation from equilibrated structures by "melt" and "soup" methods for QC calculations. Sidechains are removed in the snapshots, (an example of) targeted chain for QC calculations are shown in blue and the surrounding molecules are shown in red.

3. Results and Discussion

The electronic structure properties of SCPs are determined by the chain conformation and the electrostatic environment of the chain. Thus, the QC/MD method should accurately represent both characteristics to give reliable electronic properties. Therefore, in the first section, we analyse and compare the performance of "melt" and "soup" methods with respect to morphological properties and, in the second section, we evaluate their capabilities in predicting the electronic properties and reproducing the electrostatic environment.

3.1. Morphological properties

The first microstructural analysis is the inter-fragments torsion distribution, i.e., one of the most significant parameter on electronic properties of SCPs,[51–53] as obtained from "melt" and "soup" samples. Figure 2 (left panel) shows a comparison between the inter-repeat unit torsion distributions obtained from "melt" (filled bars) and "soup" (unfilled bars) samples, as well as the Boltzmann distribution (dashed line) calculated based on the input torsional potential (obtained from DFT scans on the repeat-unit representative molecule). As clearly shown in Figure 2 (left), the "soup" method can accurately capture the inter-monomer torsion distribution for all polymers. Figure S14 in the SI illustrates that a similar conclusion is valid for the other torsional potentials. Moreover, the deviation of torsion angle distributions obtained from MD simulations from the Boltzmann distribution quantifies the impact of surrounding molecules and sidechains and the importance of using QC/MD schemes for calculating electronic structure properties instead of using ideal chain conformations for the QC calculations. It should be emphasised that the conformation of polymer chains in bulk are also influenced by (i) the mobility confinements imposed by the connectivity of the repeat units along the polymer chain, (ii) the conformation of sidechains attached to the backbone, and (iii) the steric effect of surrounding molecules (i.e., polymers in case of "melt" and repeat units in case of "soup" models)- thus, deviations in torsion angle distribution of MD models from the Boltzmann distribution is naturally expected. Also, such deviation is expected to be larger in case of smaller torsion barriers, e.g., compare the deviation in $\phi_{2TT\text{-}2TT}$ (~ 4 k_BT) torsion in DPP-2TT polymer with $\phi_{T\text{-}DPP}$ (~ 10 k_BT) in DPP-DTT polymer in Figure 2.

The next important structural characteristic for SCPs is the chain end-to-end distance L_e and its distribution. L_e quantifies how stretched polymer chains are in bulk and it is an important property by which the robustness of "soup" method in accurate representation of SCP microstructure can be evaluated. Figure 2 (middle panel) shows the average, standard deviation from the average, and distribution of L_e for all five polymers as obtained from "melt" and "soup" samples. Note that an estimation of contour length L_c of polymers (i.e., the length of a fully stretched chain) are given on each graph. As shown, similar to the torsional distribution, the "soup" method generates very similar L_e and L_e distribution as compared to the "melt" method for all polymers. Note that the difference in the averages obtained from the two methods is well below the standard deviations obtained from "melt" simulations.

Radial distribution function (*rdf*) is another important analysis as it illustrates the inter-molecular interactions of the models. Therefore, the *rdf* of all atoms within one polymer chain with respect to all other surrounding molecules (i.e., polymer chains in case of "melt" and repeat units in case of "soup") are shown in Figure 2 (right panel). As shown, the most short-range inter-chain interactions have been captured by the "soup" method. However, the long-range orders cannot be reproduced by the "soup" method. This is, however, somehow expected due to the removal of the natural confinement imposed by the inter-repeat unit covalent bonds in surrounding polymer chains in case of "soup" models. Nevertheless, as we will see in the next section, the difference in *rdf* between "soup" and "melt" snapshots does not necessarily translate into a difference in the main quantities of merit (DOS and LL).

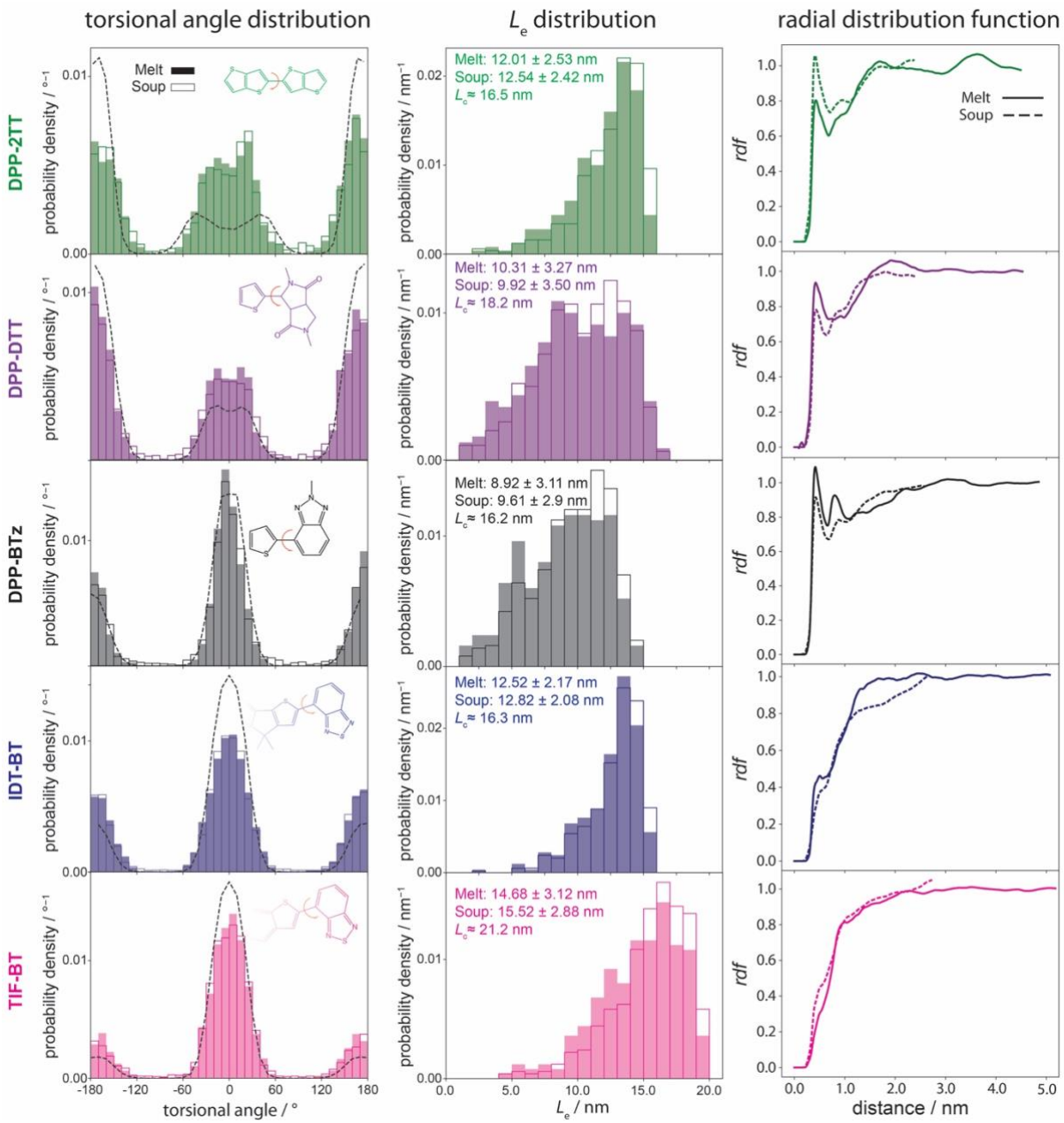

Figure 2. Torsional angle (left) and end-to-end distance L_e (middle) distributions for equilibrated polymer chains obtained from "melt", filled bars, and "soup", unfilled bars, methods. The black dashed lines show the corresponding Boltzmann distribution of torsion angles as obtained from DFT scans on the representative repeat-unit molecule. The average and standard deviation from average of L_e and contour length L_c of SCPs are given on each graph in the right panel. *rdf* ((right) of all atoms in the backbone of a polymer chain as the "reference" and the other chains (for melt simulations)/repeat units (for soup simulations) as the "surrounding" atoms. Note that the intra-molecule interactions are excluded in all *rdf* graphs.

3.2. Electronic structure properties

Figure 3 shows the DOS and LL calculated based on "melt" (solid line) and "soup" (dashed line) models. The former property is recognised as determining charge carrier mobility in amorphous semiconductors, where charge transport is modelled by variable-range hopping between localised states,[54] and the latter property (an orbital localisation measure) is hence

useful as a predictor of mobility in these materials. As can be seen, a great agreement between the two calculations exists. This indicates that the two dominant factors determining electronic structure properties, i.e., chain conformation and electrostatic environment, can be accurately captured by the "soup" method, despite some clear differences observed in the inter-chain interactions between the "melt" and "soup" samples. Although the "soup" method is generally successful in replicating the properties calculated from "melt" models, the degree of agreement between the two differs slightly for different polymers. For instance, the "soup" method gives an almost identical prediction for the DOS and LL of DPP-based polymers modelled by "melt" approach while for those containing BT as the acceptor, a larger degree of mismatch can be seen. However, the difference between polymers is considerably larger than the difference between the two methods, which, by definition, identifies the "soup" as a predictive method.

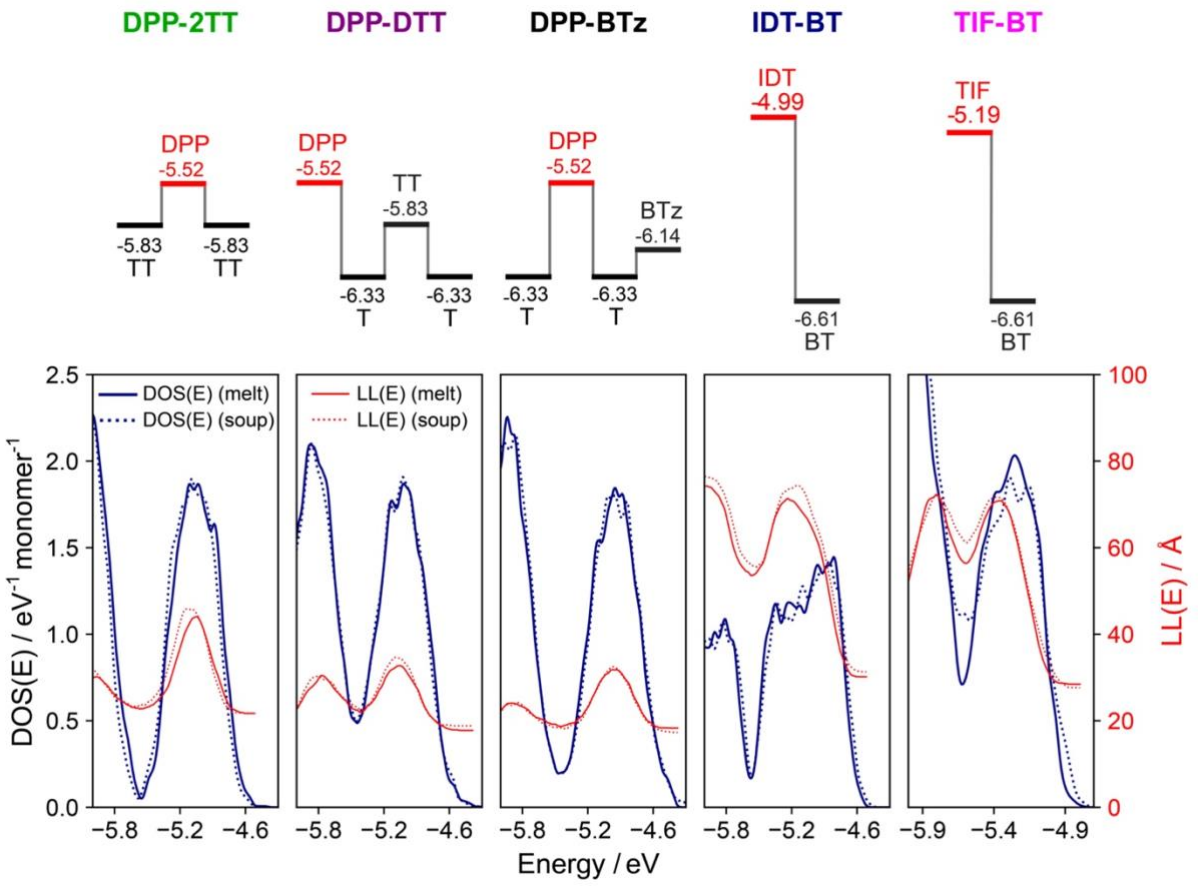

Figure 3. (top) Abbreviated names and HOMO energies of monomers for each polymer repeat unit. Separation of horizontal bars indicates separation in energy. (bottom) Density of states (DOS(E)) and localisation lengths (LL(E)) for each polymer, averaged over 250 chain conformations. DOS and LL for "melt" and "soup" models are shown with solid and dotted lines, respectively.

As discussed in the introduction, the availability of a homogenous set of simulations is helpful in extracting interesting structure-property relationships. For instance, these simulations allow the separation of the effect of the electrostatic disorder and conformational disorder on electronic structure properties of SCPs. Calculating the DOS of the five polymers in the absence of the surrounding charges (see Figure 4), we notice that the later have a very different impact on the DOS, more dramatic for DPP polymers and almost negligible for the IDT one so that the decrease in the slope of the DOS tail at the valence band edge due to the electrostatic disorder follows this order: DPP-BTz (2.20) > DPP-DTT (2.06) > DPP-2TT = TIF-BT (1.51) > IDT-BT (1.29 eV^{-2} $monomer^{-1}$).

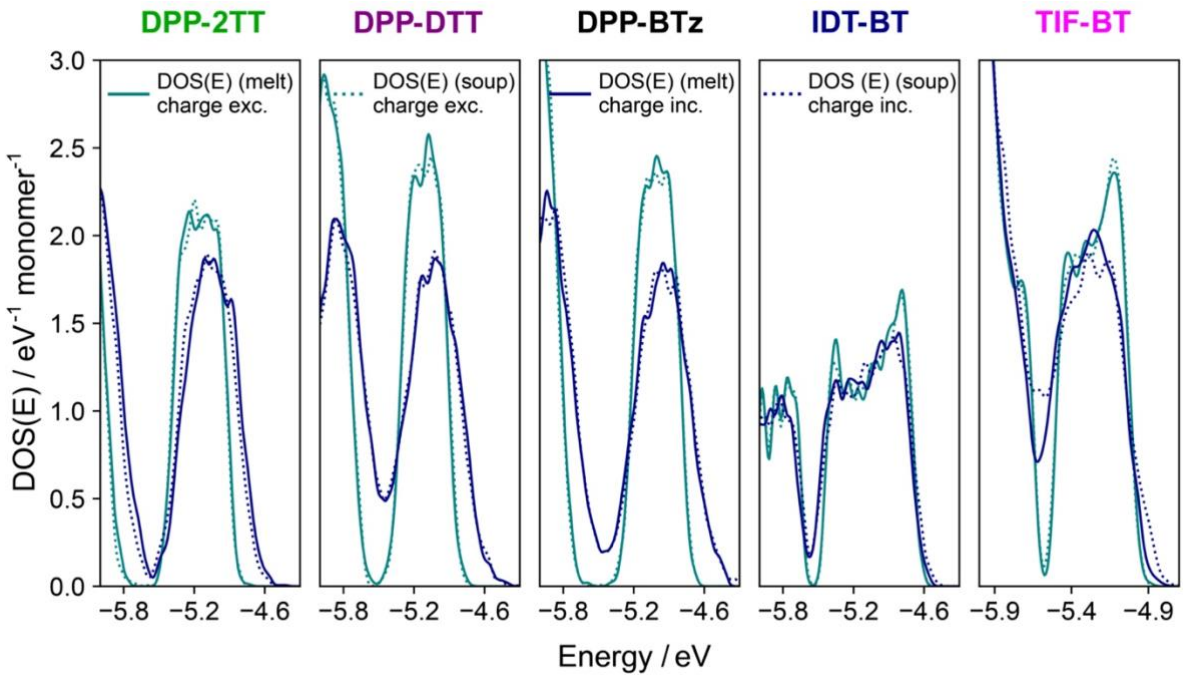

Figure 4. Energy-dependent density of states (DOS(E)) with/out electrostatic effects of the surrounding molecules, averaged over 250 chain conformations for each polymer.

This can be rationalized by looking at the variation of the electrostatic potential (EP) generated by these polymers around each chain. We have evaluated them through computing the EP disorder generated by the atoms in the repeat unit structure on a shell surrounding the repeat unit (see SI, section S3). The distribution of EPs around DPP-based polymers (standard deviation of EPs is ~ 0.60 V) is relatively wider as compared to IDT- and TIF-based ones (~ 0.40 V). Moreover, we know that the decrease in the DOS tail slope due to the environment correlates with the increase in electrostatic disorder felt by the highest HOMO monomers in each polymer (i.e., DPP, TIF, and IDT) from the surrounding molecules. To this end, we calculated the EP exerted by the surrounding molecules on a shell around DPP, TIF, and IDT

monomers for DPP-BTz, TIF-BT, and IDT-BT polymers. As expected, DPP feels the largest electrostatic disorder (0.319 V), followed by TIF (0.177 V) and IDT (0.142 V), most likely due to (i) the larger disturbance imposed by the surrounding chains and (ii) the smaller size of DPP compared to IDT and TIF. Therefore, such calculations can constitute an easy design principle to consider for the development of new materials. This is an example of how structure-property relationships are more easily derived by comparing across consistent sets of simulations.

Conclusions

In this paper, we put forward a workflow to obtain atomistic models form SCP chemical drawings. Furthermore, we suggested a simplified alternative equilibration method (i.e., "soup" method) which can predict accurately intramolecular conformations and electronic properties (density of states, localization length) of a range of polymers. Our QC/MD scheme as presented in this paper tremendously reduces calculation time from typically a few months per polymer (through manual and conventional methods) to a few days per polymer. More importantly, it enables an accurate estimation of SCP electronic structure properties with a constant calculation setup (e.g., simulation box dimension, simulation time, temperature, equilibration scheme), regardless of the polymer structure. Therefore, it will tremendously facilitate future endeavours in exploring a large space of SCPs with directly comparable methods. Last, we show that the availability of homogenous set of simulations is helpful in extracting interesting structure-property relationships, in this case: the greater effect of the surrounding polymer chains on the DOS of DPP polymers in comparison to the others.

Acknowledgement

The authors thank the support from the European Research Council (Grant No. 101020369).

Supporting Information

Force field parametrisation and model details; Equilibration and analyses details; the electrostatic disorder generated by SCP on the surrounding.

References

(1) Kim, M.; Ryu, S. U.; Park, S. A.; Choi, K.; Kim, T.; Chung, D.; Park, T. Donor–Acceptor-Conjugated Polymer for High-Performance Organic Field-Effect Transistors: A Progress Report. *Adv. Funct. Mater.* **2020**, *30* (20), 1–25. https://doi.org/10.1002/adfm.201904545.

(2) Paterson, A. F.; Singh, S.; Fallon, K. J.; Hodsden, T.; Han, Y.; Schroeder, B. C.; Bronstein, H.; Heeney, M.; McCulloch, I.; Anthopoulos, T. D. Recent Progress in High-Mobility Organic Transistors: A Reality Check. *Adv. Mater.* **2018**, *30* (36), 1–33. https://doi.org/10.1002/adma.201801079.

(3) Wang, M.; Baek, P.; Akbarinejad, A.; Barker, D.; Travas-Sejdic, J. Conjugated Polymers and Composites for Stretchable Organic Electronics. *J. Mater. Chem. C* **2019**, *7* (19), 5534–5552. https://doi.org/10.1039/c9tc00709a.

(4) Ding, L.; Yu, Z. Di; Wang, X. Y.; Yao, Z. F.; Lu, Y.; Yang, C. Y.; Wang, J. Y.; Pei, J. Polymer Semiconductors: Synthesis, Processing, and Applications. *Chem. Rev.* **2023**, *123* (12), 7421–7497. https://doi.org/10.1021/acs.chemrev.2c00696.

(5) Dang, D.; Yu, D.; Wang, E. Conjugated Donor–Acceptor Terpolymers Toward High-Efficiency Polymer Solar Cells. *Adv. Mater.* **2019**, *31* (22), 1–33. https://doi.org/10.1002/adma.201807019.

(6) Holliday, S.; Donaghey, J. E.; McCulloch, I. Advances in Charge Carrier Mobilities of Semiconducting Polymers Used in Organic Transistors. *Chem. Mater.* **2014**, *26* (1), 647–663. https://doi.org/10.1021/cm402421p.

(7) Ostroverkhova, O. Organic Optoelectronic Materials: Mechanisms and Applications. *Chem. Rev.* **2016**, *116* (22), 13279–13412. https://doi.org/10.1021/acs.chemrev.6b00127.

(8) Dimov, I. B.; Moser, M.; Malliaras, G. G.; McCulloch, I. Semiconducting Polymers for Neural Applications. *Chem. Rev.* **2022**, *122* (4), 4356–4396. https://doi.org/10.1021/acs.chemrev.1c00685.

(9) Bronstein, H.; Nielsen, C. B.; Schroeder, B. C.; McCulloch, I. The Role of Chemical Design in the Performance of Organic Semiconductors. *Nat. Rev. Chem.* **2020**, *4* (2), 66–77. https://doi.org/10.1038/s41570-019-0152-9.

(10) Omar, Ö. H.; Del Cueto, M.; Nematiaram, T.; Troisi, A. High-Throughput Virtual Screening for Organic Electronics: A Comparative Study of Alternative Strategies. *J. Mater. Chem. C* **2021**, *9* (39), 13557–13583. https://doi.org/10.1039/d1tc03256a.

(11) Terence Blaskovits, J.; Garner, M. H.; Corminboeuf, C. Symmetry-Induced Singlet-Triplet Inversions in Non-Alternant Hydrocarbons**. *Angew. Chemie - Int. Ed.* **2023**, *62* (15). https://doi.org/10.1002/anie.202218156.

(12) Omar, Ö. H.; Xie, X.; Troisi, A.; Padula, D. Identification of Unknown Inverted Singlet-Triplet Cores by High-Throughput Virtual Screening. *J. Am. Chem. Soc.* **2023**, *145* (36), 19790–19799. https://doi.org/10.1021/jacs.3c05452.

(13) Yang, Y.; Rice, B.; Shi, X.; Brandt, J. R.; Correa Da Costa, R.; Hedley, G. J.; Smilgies, D. M.; Frost, J. M.; Samuel, I. D. W.; Otero-De-La-Roza, A.; Johnson, E. R.; Jelfs, K. E.; Nelson, J.; Campbell, A. J.; Fuchter, M. J. Emergent Properties of an Organic Semiconductor Driven by Its Molecular Chirality. *ACS Nano* **2017**, *11* (8), 8329–8338. https://doi.org/10.1021/acsnano.7b03540.

(14) Nematiaram, T.; Troisi, A. Strategies to Reduce the Dynamic Disorder in Molecular Semiconductors. *Mater. Horizons* **2020**, *7* (11), 2922–2928.

https://doi.org/10.1039/d0mh01159b.
(15) Qin, T.; Troisi, A. Relation between Structure and Electronic Properties of Amorphous MEH-PPV Polymers. *J. Am. Chem. Soc.* **2013**, *135* (30), 11247–11256. https://doi.org/10.1021/ja404385y.
(16) Prodhan, S.; Manurung, R.; Troisi, A. From Monomer Sequence to Charge Mobility in Semiconductor Polymers via Model Reduction. *Adv. Funct. Mater.* **2023**, *33* (36), 1–10. https://doi.org/10.1002/adfm.202303234.
(17) Manurung, R.; Troisi, A. Screening Semiconducting Polymers to Discover Design Principles for Tuning Charge Carrier Mobility. *J. Mater. Chem. C* **2022**, *10* (38), 14319–14333. https://doi.org/10.1039/d2tc02527b.
(18) Jackson, N. E.; Kohlstedt, K. L.; Savoie, B. M.; Olvera De La Cruz, M.; Schatz, G. C.; Chen, L. X.; Ratner, M. A. Conformational Order in Aggregates of Conjugated Polymers. *J. Am. Chem. Soc.* **2015**, *137* (19), 6254–6262. https://doi.org/10.1021/jacs.5b00493.
(19) Jackson, N. E.; Savoie, B. M.; Kohlstedt, K. L.; Marks, T. J.; Chen, L. X.; Ratner, M. A. Structural and Conformational Dispersion in the Rational Design of Conjugated Polymers. *Macromolecules* **2014**, *47* (3), 987–992. https://doi.org/10.1021/ma4023923.
(20) Wilbraham, L.; Berardo, E.; Turcani, L.; Jelfs, K. E.; Zwijnenburg, M. A. High-Throughput Screening Approach for the Optoelectronic Properties of Conjugated Polymers. *J. Chem. Inf. Model.* **2018**, *58* (12), 2450–2459. https://doi.org/10.1021/acs.jcim.8b00256.
(21) Manurung, R.; Li, P.; Troisi, A. Rapid Method for Calculating the Conformationally Averaged Electronic Structure of Conjugated Polymers. *J. Phys. Chem. B* **2021**, *125* (23), 6338–6348. https://doi.org/10.1021/acs.jpcb.1c02866.
(22) Melnyk, A.; Junk, M. J. N.; McGehee, M. D.; Chmelka, B. F.; Hansen, M. R.; Andrienko, D. Macroscopic Structural Compositions of π-Conjugated Polymers: Combined Insights from Solid-State NMR and Molecular Dynamics Simulations. *J. Phys. Chem. Lett.* **2017**, *8* (17), 4155–4160. https://doi.org/10.1021/acs.jpclett.7b01443.
(23) Matta, M.; Wu, R.; Paulsen, B. D.; Petty, A. J.; Sheelamanthula, R.; McCulloch, I.; Schatz, G. C.; Rivnay, J. Ion Coordination and Chelation in a Glycolated Polymer Semiconductor: Molecular Dynamics and X-Ray Fluorescence Study. *Chem. Mater.* **2020**, *32* (17), 7301–7308. https://doi.org/10.1021/acs.chemmater.0c01984.
(24) Moro, S.; Siemons, N.; Drury, O.; Warr, D. A.; Moriarty, T. A.; Perdigão, L. M. A.; Pearce, D.; Moser, M.; Hallani, R. K.; Parker, J.; McCulloch, I.; Frost, J. M.; Nelson, J.; Costantini, G. The Effect of Glycol Side Chains on the Assembly and Microstructure of Conjugated Polymers. *ACS Nano* **2022**, *16* (12), 21303–21314. https://doi.org/10.1021/acsnano.2c09464.
(25) Roscioni, O. M.; Ricci, M.; Zannoni, C.; D'Avino, G. Are Coarse-Grained Structures as Good as Atomistic Ones for Calculating the Electronic Properties of Organic Semiconductors? *J. Phys. Chem. C* **2022**. https://doi.org/10.1021/acs.jpcc.2c08862.
(26) Makki, H.; Troisi, A. Morphology of Conducting Polymer Blends at the Interface of Conducting and Insulating Phases: Insight from PEDOT:PSS Atomistic Simulations. *J. Mater. Chem. C* **2022**, *10* (42), 16126–16137. https://doi.org/10.1039/d2tc03158b.
(27) Makki, H.; Burke, C. A.; Troisi, A. Microstructural Model of Indacenodithiophene-Co-Benzothiadiazole Polymer: Π-Crossing Interactions and Their Potential Impact on Charge Transport. *J. Phys. Chem. Lett.* **2023**, *14*, 8867–8873.

https://doi.org/10.1021/acs.jpclett.3c02305.
(28) Venkateshvaran, D.; Nikolka, M.; Sadhanala, A.; Lemaur, V.; Zelazny, M.; Kepa, M.; Hurhangee, M.; Kronemeijer, A. J.; Pecunia, V.; Nasrallah, I.; Romanov, I.; Broch, K.; McCulloch, I.; Emin, D.; Olivier, Y.; Cornil, J.; Beljonne, D.; Sirringhaus, H. Approaching Disorder-Free Transport in High-Mobility Conjugated Polymers. *Nature* **2014**, *515* (7527), 384–388. https://doi.org/10.1038/nature13854.
(29) Jackson, J. K.; Rosa, E. De; Winter, H. Molecular Weight Dependence of Relaxation Time Spectra for the Entanglement and Flow Behavior of Monodisperse Linear Flexible Polymers. *Macromolecules* **1994**, *27*, 2426–2431.
(30) Botiz, I.; Durbin, M. M.; Stingelin, N. Providing a Window into the Phase Behavior of Semiconducting Polymers. *Macromolecules* **2021**, *54* (12), 5304–5320. https://doi.org/10.1021/acs.macromol.1c00296.
(31) Cheung, D. L.; McMahon, D. P.; Troisi, A. A Realistic Description of the Charge Carrier Wave Function in Microcrystalline Polymer Semiconductors. *J. Am. Chem. Soc.* **2009**, *131* (31), 11179–11186. https://doi.org/10.1021/ja903843c.
(32) Avino, G. D.; Muccioli, L.; Zannoni, C.; Wang, L.; Beljonne, D. Energetics of Electron − Hole Separation at P3HT / PCBM Heterojunctions. *J. Phys. Chem. C* **2013**, *117*, 12981–12990. https://doi.org/https://doi.org/10.1021/jp402957g.
(33) Heck, A.; Kranz, J. J.; Elstner, M. Simulation of Temperature-Dependent Charge Transport in Organic Semiconductors with Various Degrees of Disorder. *J. Chem. Theory Comput.* **2016**, *12* (7), 3087–3096. https://doi.org/10.1021/acs.jctc.6b00215.
(34) McMahon, D. P.; Troisi, A. An Ad Hoc Tight Binding Method to Study the Electronic Structure of Semiconducting Polymers. *Chem. Phys. Lett.* **2009**, *480* (4–6), 210–214. https://doi.org/10.1016/j.cplett.2009.09.032.
(35) Schütze, Y.; Gayen, D.; Palczynski, K.; de Oliveira Silva, R.; Lu, Y.; Tovar, M.; Partovi-Azar, P.; Bande, A.; Dzubiella, J. How Regiochemistry Influences Aggregation Behavior and Charge Transport in Conjugated Organosulfur Polymer Cathodes for Lithium-Sulfur Batteries. *ACS Nano* **2023**, *17* (8), 7889–7900. https://doi.org/10.1021/acsnano.3c01523.
(36) Yan, X. 2018_Pnas_Si_Spe. *Proc. Natl. Acad. Sci.* **2017**, *120*, 2017. https://doi.org/10.1073/pnas.
(37) Lemaur, V.; Cornil, J.; Lazzaroni, R.; Sirringhaus, H.; Beljonne, D.; Olivier, Y. Resilience to Conformational Fluctuations Controls Energetic Disorder in Conjugated Polymer Materials: Insights from Atomistic Simulations. *Chem. Mater.* **2019**, *31* (17), 6889–6899. https://doi.org/10.1021/acs.chemmater.9b01286.
(38) Sears, J. S.; Chance, R. R.; Brédas, J. L. Torsion Potential in Polydiacetylene: Accurate Computations on Oligomers Extrapolated to the Polymer Limit. *J. Am. Chem. Soc.* **2010**, *132* (38), 13313–13319. https://doi.org/10.1021/ja103769j.
(39) Jorgensen, W. L.; Maxwell, D. S.; Tirado-Rives, J. Development and Testing of the OPLS All-Atom Force Field on Conformational Energetics and Properties of Organic Liquids. *J. Am. Chem. Soc.* **1996**, *118* (45), 11225–11236. https://doi.org/10.1021/ja9621760.
(40) Wang, J.; Wolf, R. M.; Caldwell, J. W.; Kollman, P. A.; Case, D. A. Development and Testing of a General Amber Force Field. *J. Comput. Chem.* **2004**, *25* (9), 1157–1174. https://doi.org/10.1002/jcc.20035.
(41) Cheung, D. L.; Mcmahon, D. P.; Troisi, A. Computational Study of the Structure and Charge-Transfer Parameters in Low-Molecular-Mass P3HT. *J. Phys. Chem. B* **2009**, *113*

(28), 9393–9401. https://doi.org/10.1021/jp904057m.
(42) Cacelli, I.; Prampolini, G. Parametrization and Validation of Intramolecular Force Fields Derived from DFT Calculations. *J. Chem. Theory Comput.* **2007**, *3* (5), 1803–1817. https://doi.org/10.1021/ct700113h.
(43) Grimme, S. A General Quantum Mechanically Derived Force Field (QMDFF) for Molecules and Condensed Phase Simulations. *J. Chem. Theory Comput.* **2014**, *10* (10), 4497–4514. https://doi.org/10.1021/ct500573f.
(44) Claridge, K.; Troisi, A. Developing Consistent Molecular Dynamics Force Fields for Biological Chromophores via Force Matching. *J. Phys. Chem. B* **2019**, *123* (2), 428–438. https://doi.org/10.1021/acs.jpcb.8b10746.
(45) Michaels, W.; Zhao, Y.; Qin, J. Atomistic Modeling of PEDOT:PSS Complexes II: Force Field Parameterization. *Macromolecules* **2021**, *54* (12), 5354–5365. https://doi.org/10.1021/acs.macromol.1c00860.
(46) Keene, S. T.; Michaels, W.; Melianas, A.; Quill, T. J.; Fuller, E. J.; Giovannitti, A.; McCulloch, I.; Talin, A. A.; Tassone, C. J.; Qin, J.; Troisi, A.; Salleo, A. Efficient Electronic Tunneling Governs Transport in Conducting Polymer-Insulator Blends. *J. Am. Chem. Soc.* **2022**, *144* (23), 10368–10376. https://doi.org/10.1021/jacs.2c02139.
(47) Patrone, P. N.; Dienstfrey, A.; Browning, A. R.; Tucker, S.; Christensen, S. Uncertainty Quantification in Molecular Dynamics Studies of the Glass Transition Temperature. *Polymer (Guildf).* **2016**, *87*, 246–259. https://doi.org/10.1016/j.polymer.2016.01.074.
(48) Hopkins, C. W.; Le Grand, S.; Walker, R. C.; Roitberg, A. E. Long-Time-Step Molecular Dynamics through Hydrogen Mass Repartitioning. *J. Chem. Theory Comput.* **2015**, *11* (4), 1864–1874. https://doi.org/10.1021/ct5010406.
(49) Omar, Ö. H.; Nematiaram, T.; Troisi, A.; Padula, D. Organic Materials Repurposing, a Data Set for Theoretical Predictions of New Applications for Existing Compounds. *Sci. Data* **2022**, *9* (1), 1–8. https://doi.org/10.1038/s41597-022-01142-7.
(50) Thomas, T. H.; Harkin, D. J.; Gillett, A. J.; Lemaur, V.; Nikolka, M.; Sadhanala, A.; Richter, J. M.; Armitage, J.; Chen, H.; McCulloch, I.; Menke, S. M.; Olivier, Y.; Beljonne, D.; Sirringhaus, H. Short Contacts between Chains Enhancing Luminescence Quantum Yields and Carrier Mobilities in Conjugated Copolymers. *Nat. Commun.* **2019**, *10* (1). https://doi.org/10.1038/s41467-019-10277-y.
(51) Yan, X.; Xiong, M.; Deng, X. Y.; Liu, K. K.; Li, J. T.; Wang, X. Q.; Zhang, S.; Prine, N.; Zhang, Z.; Huang, W.; Wang, Y.; Wang, J. Y.; Gu, X.; So, S. K.; Zhu, J.; Lei, T. Approaching Disorder-Tolerant Semiconducting Polymers. *Nat. Commun.* **2021**, *12* (1), 1–9. https://doi.org/10.1038/s41467-021-26043-y.
(52) Kanimozhi, C.; Naik, M.; Yaacobi-Gross, N.; Burnett, E. K.; Briseno, A. L.; Anthopoulos, T. D.; Patil, S. Controlling Conformations of Diketopyrrolopyrrole-Based Conjugated Polymers: Role of Torsional Angle. *J. Phys. Chem. C* **2014**, *118* (22), 11536–11544. https://doi.org/10.1021/jp501526h.
(53) Darling, S. B. Isolating the Effect of Torsional Defects on Mobility and Band Gap in Conjugated Polymers. *J. Phys. Chem. B* **2008**, *112* (30), 8891–8895. https://doi.org/10.1021/jp8017919.
(54) Tessler, N.; Preezant, Y.; Rappaport, N.; Roichman, Y. Charge Transport in Disordered Organic Materials and Its Relevance to Thin-Film Devices: A Tutorial Review. *Adv. Mater.* **2009**, *21* (27), 2741–2761. https://doi.org/10.1002/adma.200803541.